

Delineating coal seams and establishing water tightness by electrical resistivity imaging

Ch. Subba Rao*, M. Majumder, J. Roy, M. S. Chaudhari and R. S. Ramteke

Geophysics Division, Central Water and Power Research Station, Khadakwasla R.S., Pune 411 024, India

In the present study, continuity of coal seams was established in the area adjacent to the existing open cast coal mine at Talabira, Odisha situated close to Hira-kud reservoir. Water tightness of the strata in the zone between the reservoir and the mine needs to be verified to prevent inundation by subterranean seepage and ensure safety. Multi electrode resistivity imaging technique was used to establish continuity of coal seams and verify water tightness. From the studies conducted in and around the mine along 13 profiles, coal seams with relatively high resistivity ranging from 500 to 1500 Ohm-m at depths varying from 10 to 31 m were delineated. The intervening strata between the reservoir and the open cast mine was found to be fairly tight without any significant zone susceptible to seepage.

Keywords: Coal seam, electrical resistivity imaging, open cast mine, reservoir, water tightness.

TALABIRA-1 coal mine block, covering an area of about 2.6 sq. km, is in the southeastern part of the Ib River Coalfield, Sambalpur district, Odisha¹. The area lies between 21°43'42.32"–21°44'8.31" lat. and 83°58'44.03"–83°59'39.65" long. It is featured in the Survey of India toposheet no. 64 O/14. Mining is being carried out presently by continuous surface miner and Ripper-Dozer at reduced level (RL) 137 m (ref. 2). Fresh mining is proposed in a 7.05 ha area adjacent to the present mine. Some water seepage was observed in the rainy season into the open cast mine from its southern face. Electrical resistivity imaging (ERI) technique was employed to detect the quality of watertight screen in the slope of an open-pit mine³, to delineate air-filled voids within compact limestone environment which could induce collapse of roads or buildings that overlie the voids⁴, to map karst features at the location of a township site⁵, to monitor ingress of solute plumes and to detect preferential flow paths within the dry coal ash medium⁶.

As the Hira-kud reservoir is situated to the south of the mine (Figure 1), delineating and sealing the potential seepage paths, if any, from the reservoir into the mine is essential to ensure water tightness of the intervening strata to prevent inundation and consequent losses. Resistivity of earth materials is affected by the resistivity of

pore fluid, the clay content, temperature and salinity of water⁷. Multi-electrode resistivity imaging studies are useful for obtaining high-resolution, reliable subsurface resistivity images that can be interpreted in terms of geological formations⁸. Pseudosections of electrical resistivity with dense sampling depicting resistivity variations in shallow depths (0–100 m) are obtained by resistivity imaging⁹. Ratnakumari *et al.*¹⁰ have used the ERI technique for delineating deep aquifers in hard-rock areas. Krishnamurthy *et al.*¹¹ have delineated coal seam barrier thickness and demarcated water-filled voids using ERI technique. High-resistive coal seams with respect to the surrounding formations at Jharia Coalfield, Dhanbad, Jharkhand were delineated by Verma and Bhuin¹². Variation of resistivity values of coal samples of Jharia Coalfield with water saturation has been studied in the laboratory by Verma *et al.*¹³. ERI was used for detecting the quality of watertight screen in the north slope of Gushan open-pit mine, Dangtu county, Anhui province, China³. Singh *et al.*¹⁴ have employed the ERI technique for exploration of coal seams at East Basuria Colliery of Jharia Coalfield. In the present work, ERI technique was employed at Talabira to delineate (i) coal seams in the area adjacent to the present mine and (ii) potential seepage paths, if any, from the reservoir into the mine so as to enable plugging them and thus ensure safety.

The Ib River Coalfield is located in the southeastern part of the NW–SE trending Mahanadi master Basin between 21°30'–22°06'N and 83°37'–84°10'E. It covers an area of 141,587 sq. km and includes Hingir Basin in the north and Rampur Basin in the south¹⁵. Geology of the area has been worked out in detail by a number of workers. The entire Lower Gondwana succession of the Mahanadi Basin comprises Talchir, Karharbari, Barakar, Barren Measures and Raniganj (Lower Kamthi) formations¹⁶.

The geological sequence in the Talabira block-1 comprises alluvium of recent age underlain by fine to coarse-grained sandstone, carbonaceous shale, grey shale, fireclay and coal seams belonging to the Barakar Formation. These are further underlain by fine to coarse and gritty sandstone, grey shale and coal seams belonging to the Karharbari Formation. These formations are situated above fine- to medium-greenish sandstones of Talchir Formation above the basement granite gneiss¹⁷. Figure 1 shows various surface geological formations, the periphery of the Hira-kud reservoir and Talabira block-I coal area.

ERI involves a series of resistivity measurements with different electrode spacings using a 2D multielectrode imaging system to control the measurements. Increasing the electrode separation provides information regarding greater depths. The measured apparent resistivities are processed and interpreted to provide an image of the true resistivity against depth. Resistivity measurement helps in correlating the resistivity of the coal-bearing formations as seen from the exposed mine face as well as from the available bore log data. Resistivity information is also

*For correspondence. (e-mail: chilukuri3_2000@yahoo.com)

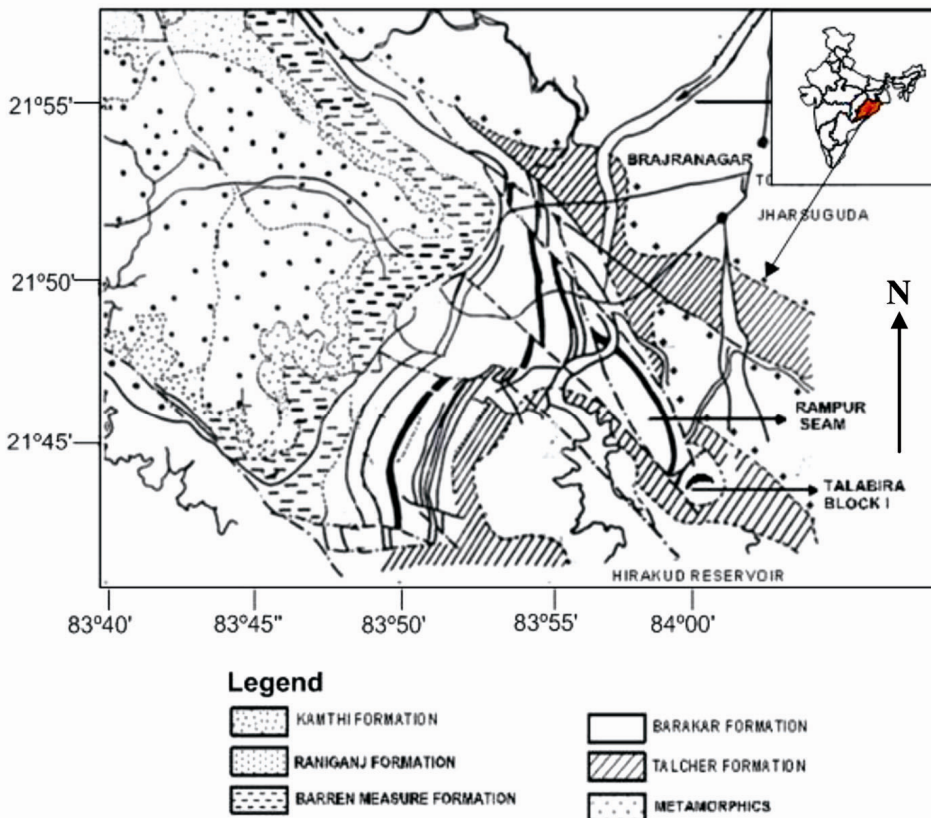


Figure 1. Geological map of Talabira coal mine and its surroundings (modified after geological report by CMPDIL, Ranchi¹⁷).

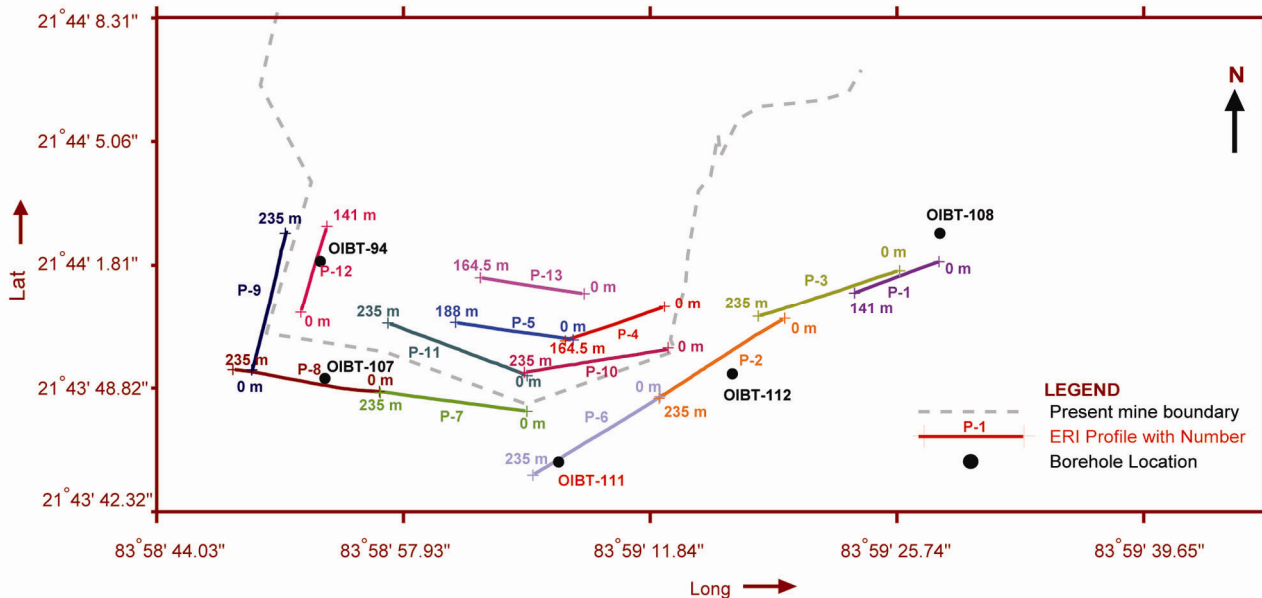


Figure 2. Location map showing electrical resistivity imaging profiles in Talabira block-1 coal mine.

useful in detecting saturated/seepage zones by indicating relatively low resistivity zones in the analysed sections.

The ERI survey was conducted using ARES automatic resistivity imaging system (M/s GF Instruments, Czech Republic). The system has a power output of 300 W and

can transmit very high currents of up to 2 A into the ground. Six multi-core cables each with 8 electrode takeouts with maximum spacing of 5.0 m were used for connecting 48 electrodes. The equipment comprises an electrode selector and an inbuilt switching unit to

Table 1. Start, end, length and coordinates of the centres of the profiles

Profile no.	Profile (m)		Length of profile (m)	Coordinates of the centre of the profile	
	From	To			
P-1	0	141	141	83°58'50.77"	21°43'53.47"
P-2	0	235	235	83°58'52.66"	21°43'48.97"
P-3	0	235	235	83°58'53.16"	21°43'54.83"
P-4	0	164.5	164.5	83°59'0.47"	21°43'47.78"
P-5	0	188	188	83°59'1"	21°43'50.59"
P-6	0	235	235	83°59'5.41"	21°43'51.38"
P-7	0	235	235	83°59'9.11"	21°43'53.83"
P-8	0	235	235	83°59'9.12"	21°43'49.72"
P-9	0	235	235	83°59'10.09"	21°43'45.87"
P-10	0	235	235	83°59'16"	21°43'51.63"
P-11	0	235	235	83°59'22.2"	21°43'49.76"
P-12	0	141	141	83°59'26.09"	21°43'52.96"
P-13	0	164.5	164.5	83°59'4.42"	21°43'53.86"

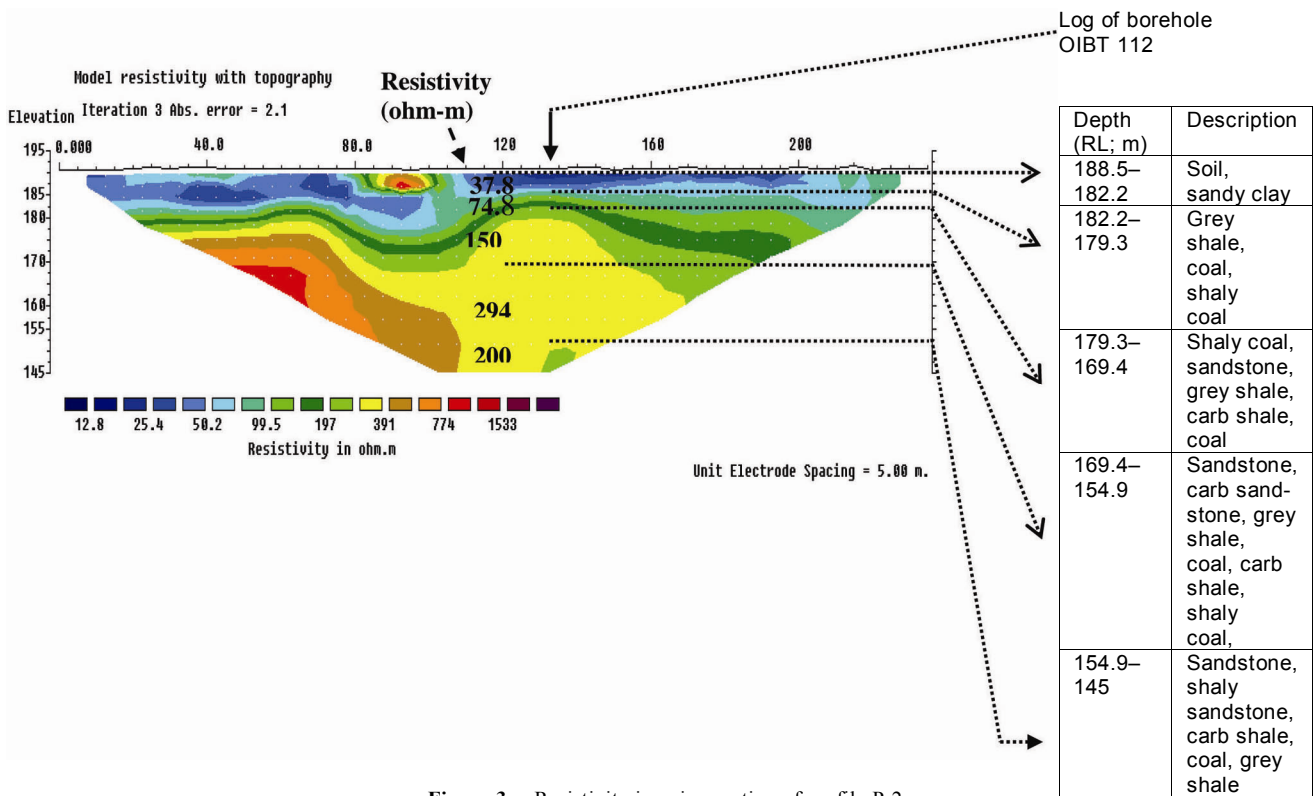


Figure 3. Resistivity imaging section of profile P-2.

select the appropriate electrodes for automatic measurement.

The survey was conducted along 13 profiles, out of which 3 (P-1, P-2 and P-3) were taken in the proposed study area for mining to verify the presence of the coal seams in this area. Three sets of parallel profiles, viz. (i) P-7, P-8, P-11, P-5 and P-13 southwest of the mine, (ii) P-6, P-10 and P-4 south of the mine parallel to the earthen embankment and (iii) P-9 and P-12 to the west of the mine were taken for delineating seepage paths, if any,

from the reservoir area into the mine. Continuity of a potential seepage path, if any, was sought to be established by the occurrence of low-resistive zones in parallel sections.

Forty-eight electrodes were planted in each profile at intervals of 3.0, 3.5, 4 or 5 m depending on the space available. This gives profile lengths of 141, 164.5, 188 or 235 m respectively. Thus, all possible routes of seepage from the reservoir into the present mining area were covered by the study (Figure 2). Table 1 depicts the start, end, length and coordinates of the centres of the profiles.

Log of borehole OIBT-108 about 100 m away from the zero chainage of profile P-3

Depth (RL; m)	Description
193.3–181.1	Sandy soil, ferruginous clay, sandstone
181.1–172.8	carb shale, coal, sandstone
172.8–162.6	Grey shale, coal, sandstone
162.6–156.8	Sandstone with coal streaks, carb shale
156.8–148.3	Grey shale, coal

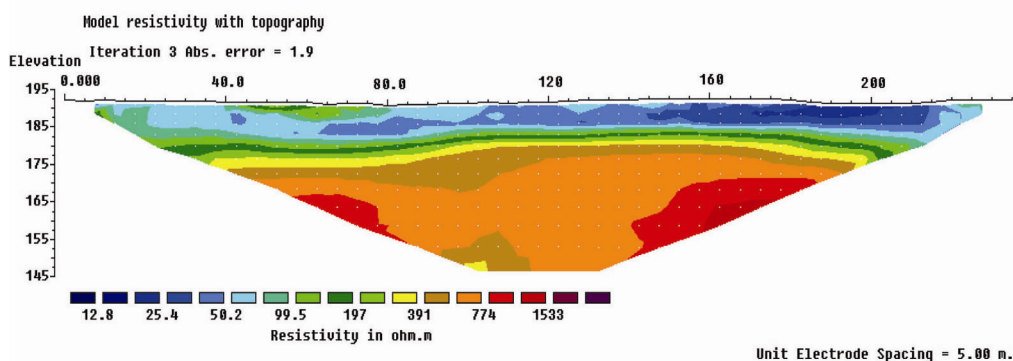


Figure 4. Resistivity imaging section of profile P-3.

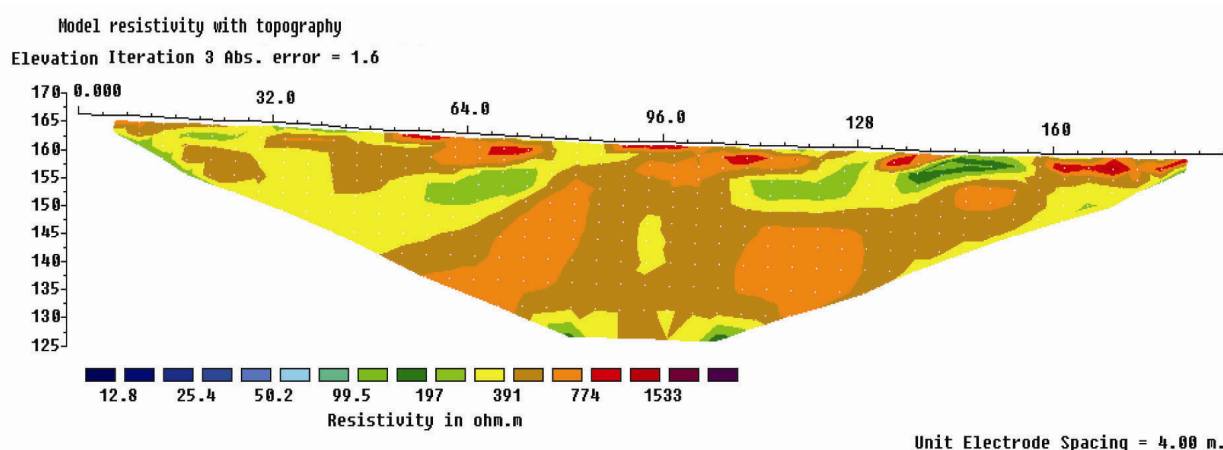


Figure 5. Resistivity imaging section of profile P-5.

The modelling has been done in two parts. A forward modelling subroutine was used to calculate the apparent resistivity values and a nonlinear least squares optimization technique and finite element method were used for the inversion routine. The inversion routine used by the RES2DINV program is based on smoothness constrained least squares technique^{18–21}. An advantage of this method is that the damping factor and flatness filter can be adjusted to suit different types of data²². This program is based on a new adoption of least squares technique, i.e. a quasi-Newton optimization technique¹⁹, which is suitable for large datasets. For the Wenner–Schlumberger configuration, the thickness of the first layer of the blocks was set at 0.5 times the electrode spacing.

Pseudosection contouring method was used to plot the data from a 2D imaging survey. The pseudo depth value is based on the sensitivity values or Fréchet derivative for

a homogeneous half space²³. The plot obtained by contouring the apparent resistivity values is a convenient means to display the data. The pseudosection gives an approximate picture of the true subsurface resistivity distribution. When the measured resistivity data are fed to the processing software, after the set number of iterations, the display shows measured apparent resistivity pseudosection, calculated apparent resistivity pseudosection and inverse model resistivity section or true resistivity section. In this communication only true resistivity sections are discussed.

A low resistive zone is shown in Figure 3 (profile P-2) from RL 190 to 170 m along the entire chainage with resistivity varying from 12.8 to 100 Ohm-m. This low resistive zone corresponds to a mixture of sandy clay and grey shale as inferred from the borehole (OIBT 112) data located close to this profile. A relatively high resistive

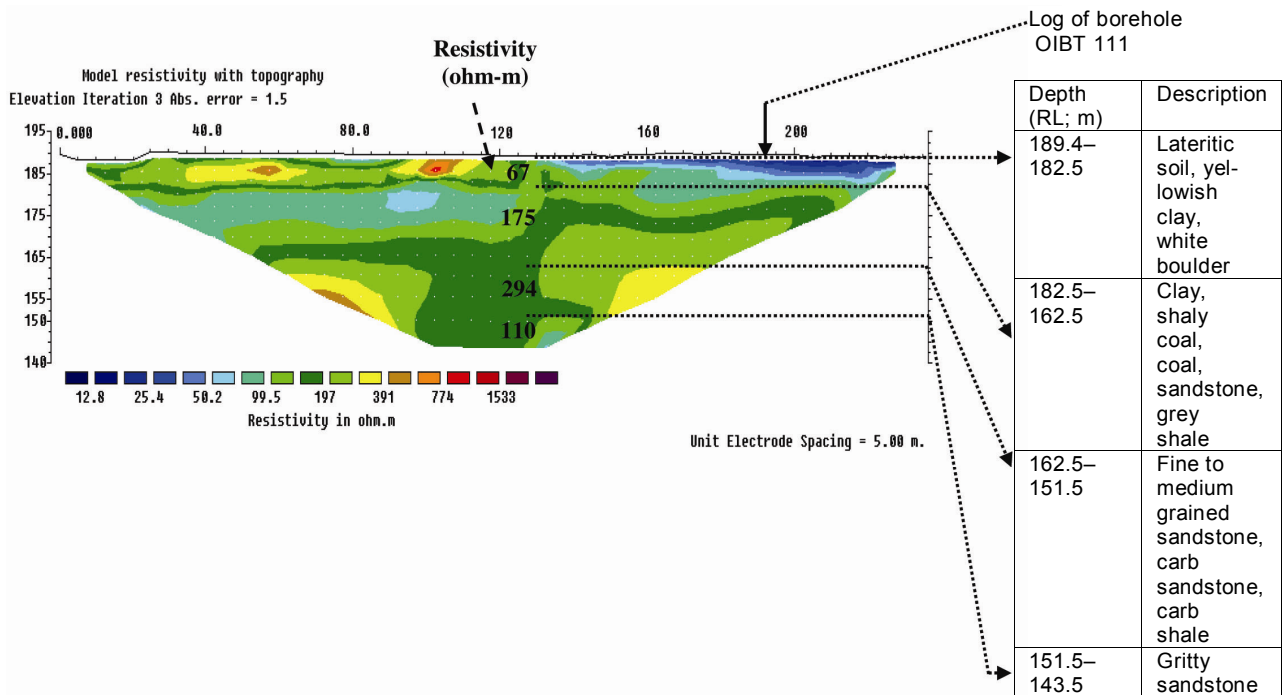


Figure 6. Resistivity imaging section of profile P-6.

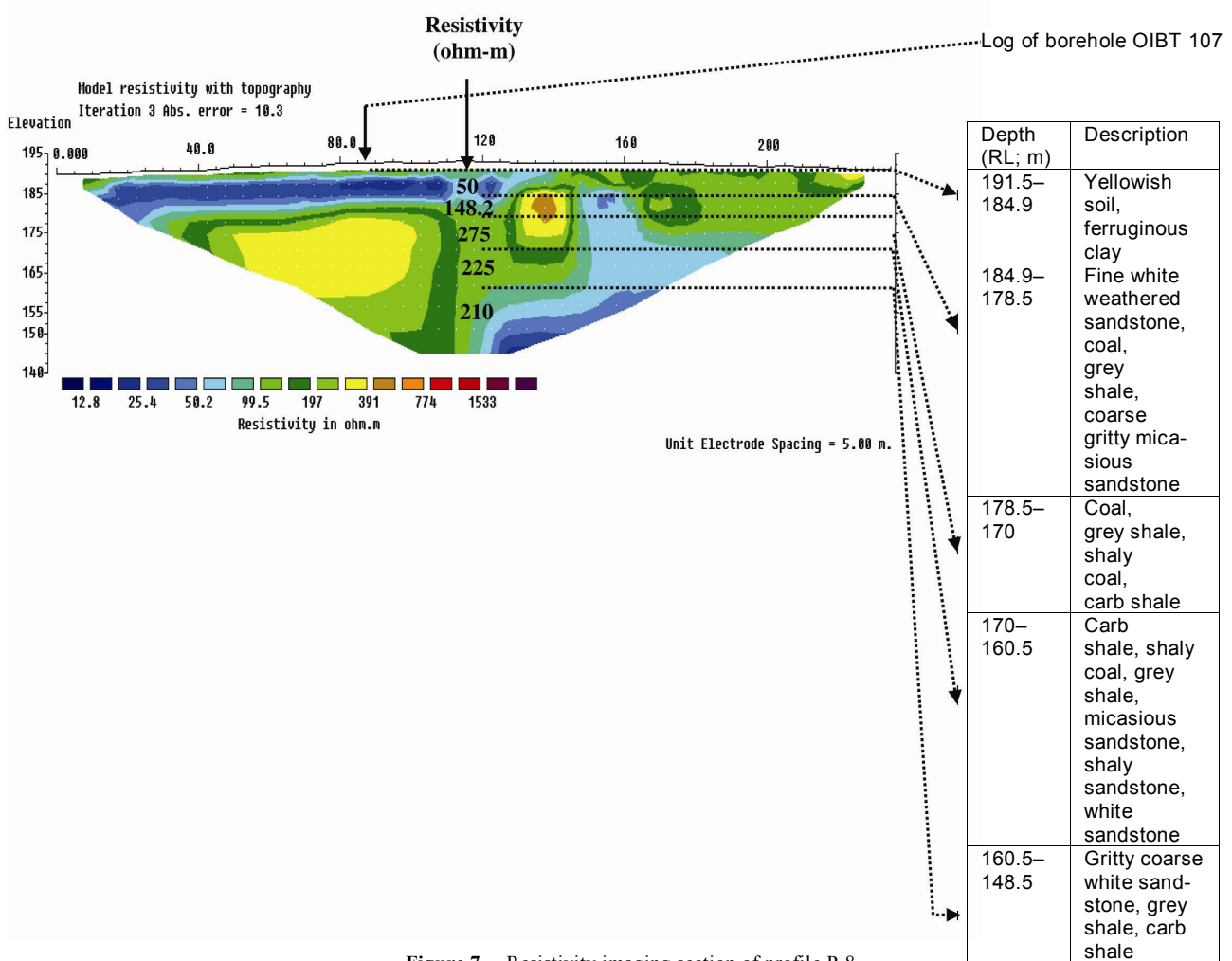


Figure 7. Resistivity imaging section of profile P-8.

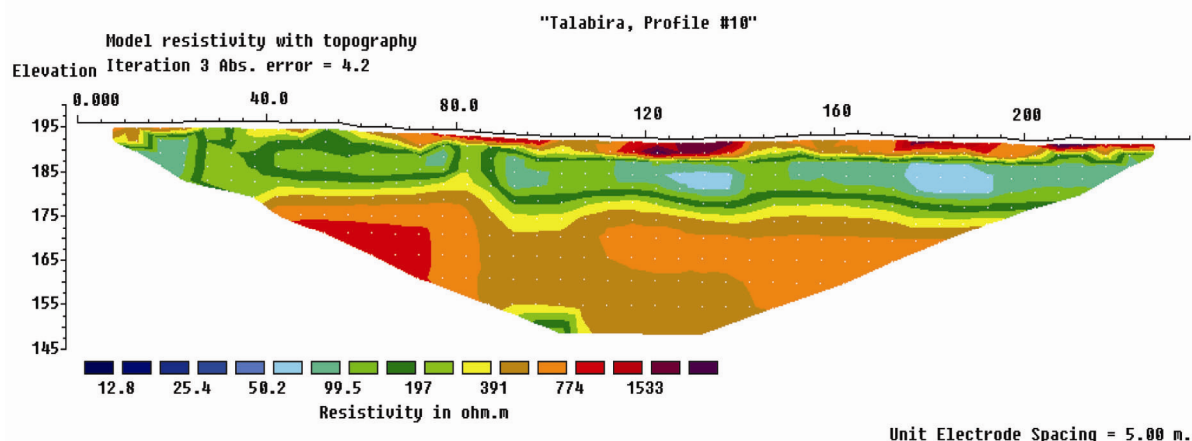


Figure 8. Resistivity imaging section of profile P-10.

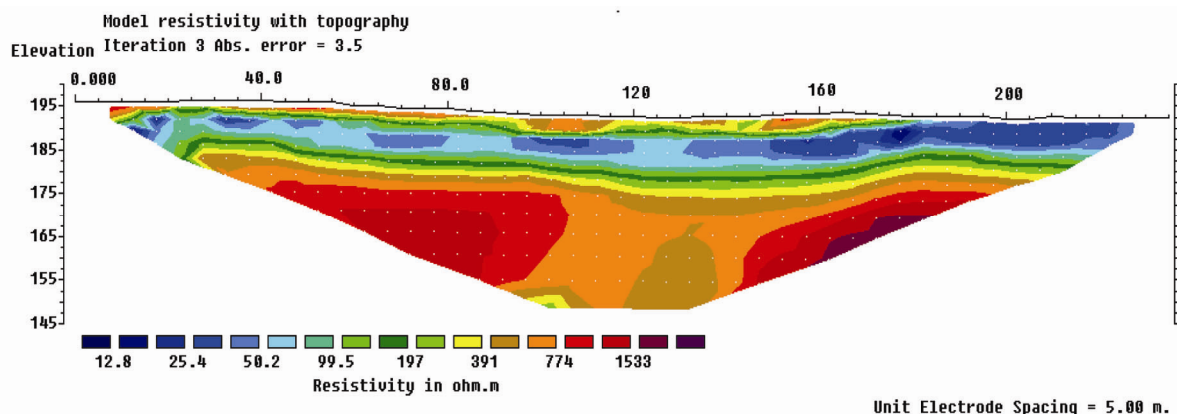


Figure 9. Resistivity imaging section of profile P-11.

zone with resistivity nearly 500–800 Ohm-m from RL 170 to 155 m was observed from chainage 30 to 110 m corresponding to the resistivity of visible coal seams in the face of the mine.

Figure 4 is the true resistivity pseudosection beneath profile P-3 situated on the proposed mining area to the north of the road. A zone between RL 179 to 145 m with resistivity ranging between 580 Ohm-m and 1500 Ohm-m is found below this profile. This range of resistivity corresponds to those obtained for coal seams in the profiles P-11 and P-12 situated right above the visible coal seams. The log of borehole OIBT-108 situated about 100 m from the zero chainage of profile P-3 along with the lithological units is presented alongside the resistivity image.

In profile P-5 (Figure 5), taken inside the mine, the substrata resistivity varies from 300 to 1100 Ohm-m, which corresponds to the resistivity of coal seams in the near vicinity.

The top surface at profile P-6 (Figure 6) is occupied by saturated lateritic soil and clay. The strata up to RL 143 m was filled with carbonaceous shale, shaly coal, fine to medium-grained sandstone as seen from borehole

(OIBT 111) data, situated on profile P-6 with low resistivity varying from 50 to 200 Ohm-m.

A low-resistive zone with resistivity of 50–150 Ohm-m is visible in profile P-8 (Figure 7) from RL 190 to 180 m on the surface corresponding to saturated clay, weathered sandstone and sandy shale as seen from borehole (OIBT 107) data. A similar low resistive zone is seen in profile P-12 from RL 193 to 185 m along the entire stretch of the profile. Clays with widely varying resistivities were reported by several authors^{24–28}. Seemingly, the low resistivity is due to saturated clay and there is no seepage path between P-8, P-9 and P-12. However, a large low-resistive zone is seen from RL 175 to 145 m in profile P-8 along the surface chainage 120 to 190 m. This zone corresponds to shaly sandstone, shaly coal, coal and coarse to fine-grained sandstone. At greater depths, the strata are dominated by sandstone. Continuity of the zone at this level has not been observed in profile P-12.

A low resistive zone is seen in profile P-10 (Figure 8) from RL 190 to RL 183 m with resistivity range from 50 to 200 Ohm-m along the entire length of the section. A thin relatively higher resistive layer with resistivity ranging

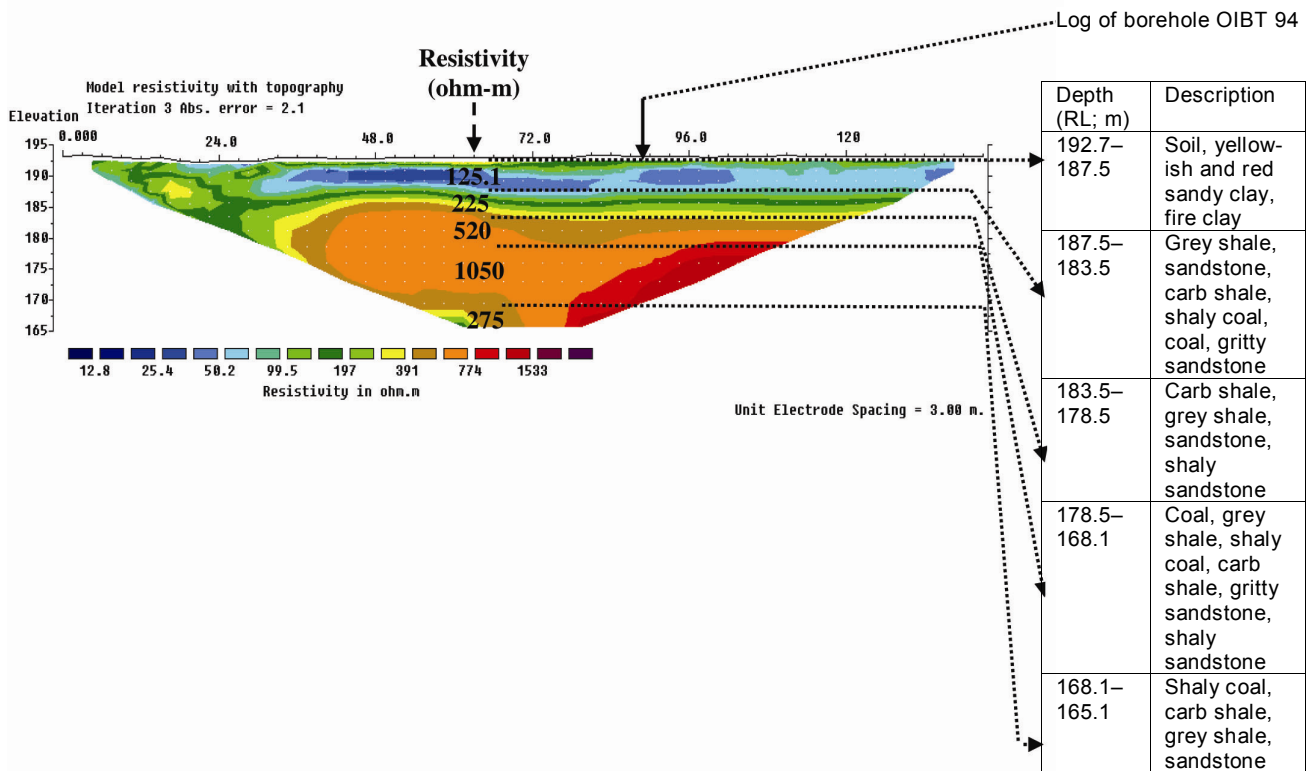


Figure 10. Resistivity imaging section of profile P-12.

from 400 to 1500 Ohm-m is seen on the surface of profile P-10 from chainage 60 to 235 m, which might represent artificially dumped material noted at the site. A small, isolated, low-resistive patch is found on profile P-10 from a depth of RL 147 to 152 m and surface chainage 95 to 105 m with a resistivity range 50–150 Ohm-m. A high-resistivity zone with resistivity varying from 500 to 1500 Ohm-m is observed from RL 180 to 145 m along the complete length of the profile corresponding to resistivity of coal seams observed in other profiles.

The top layers under profiles P-11 and P-12 (Figures 9 and 10), correspond to clay and shale layers and do not suggest any saturated zone. The underlying strata in both these profiles correspond to a series of shaly coal, sandstone and carb shale layers. Chatterjee and Paul²⁹ have reported resistivities of coal-bearing formations varying from 500 to 1200 Ohm-m. Verma and Bhui³⁰ have found a resistivity range of 989–1632 Ohm-m for coal seams at Jharia Coalfield. Therefore, near Talabira block-1 coal mine, the higher resistive zones with resistivity varying from 400 to 1500 Ohm-m observed in profiles P-11 and P-12 were inferred to be coal-bearing formations.

The higher resistivity values of about 580 to 1500 Ohm-m obtained beneath profile P-3 in the area adjacent to the present mine correspond to those of coal-bearing formations. Similar values were obtained in profiles P-10, P-11 and P-12, indicating the presence of coal

seams which is confirmed by borehole data. These formations under profile P-3 are possibly the extensions of coal seams observed in nearby profiles. The analysis of the resistivity imaging sections taken along the three sets of parallel lines (P-7, P-8, P-11, P-5 and P-13; P-6, P-10 and P-4; P-9 and P-12) revealed a few relatively low-resistive zones. These zones were correlated with coarse to fine shaly and gritty sandstone, broken shaly coal layers as reported in the boreholes situated near the profiles. A low resistive zone observed under profile P-8, though significant, does not show any continuity either in profile P-11 or P-12. Thus, there do not seem to be significant zones susceptible to seepage in the area studied.

1. <http://www.dowrorissa.gov.in/BasinMaps/MahanadiBasin.htm>
2. Basak, N. A., *Surveying and Leveling*, Tata McGraw-Hill, 1994, pp. 49–133.
3. Wusheng, H., Sijing, C. and Wenxiao, W., Images of high density resistivity method in leakage detecting of the watertight screen at Gushan open-pit mine. In Proceedings of the 2nd International Conference on Systems Engineering and Modeling (ICSEM-13), 2013.
4. Louis, L. F., Louis, F. I. and Bastou, M., Accurate subsurface characterization for highway applications using resistivity inversion methods. *J. Electr. Electron. Eng., Spec. Issue*, 2002, 43–55.
5. Elawadi, E., Gad, El-Qady, Nigm, A., Shaaban, F. and Ushijima, K., *Integrated Geophysical Survey for Site Investigation at a New Dwelling Area*, Egypt, 2006, pp. 249–259.

6. Muchingami, I., Nel, J., Xu, Y., Steyl, G. and Reynolds, K., On the use of electrical resistivity methods in monitoring infiltration of salt fluxes in dry coal ash dumps in Mpumalanga, South Africa. *Water SA*, 2013, **39**(4), 491–498.
7. William, K. F., Waller, M. J. and Layson, H. R., Monitoring moisture migration in the Vadose zone with resistivity. *Ground Water*, 1987, **25**(5), 562–571.
8. Griffiths, D. H. and Barker, R. D., Two-dimensional resistivity imaging and modeling in areas of complex geology. *J. Appl. Geophys.*, 1993, **29**, 211–226.
9. Loke, M. H. and Barker, R. D., Rapid least-square inversion of apparent resistivity pseudosections by a quasi-Newton method. *Geophys. Prospect.*, 1996, **44**, 131–152.
10. Ratnakumari, Y., Rai, S. N., Thiagarajan, S. and Dewashish Kumar, 2D electrical resistivity imaging for delineation of deeper aquifers in a part of the Chandrabhaga river basin, Nagpur District, Maharashtra, India. *Curr. Sci.*, 2012, **102**(1), 2012, 61–69.
11. Krishnamurthy, N. S., Ananda Rao, V., Dewashish Kumar, Singh, K. K. K. and Shakeel, A., Electrical resistivity imaging technique to delineate coal seam barrier thickness and demarcate water filled voids. *J. Geol. Soc. India*, 2009, **73**, 639–650.
12. Verma, R. K. and Bhui, N. C., Use of electrical resistivity methods for study of coal seams in parts of Jharia coal field, India. *Geoexploration*, 1979, **17**, 163–176.
13. Verma, R. K., Bhui, N. C. and Handu, S. K., Study of the resistivity of coal seams of the Jharia Coalfield, India. *Energy Sources*, 1982, **6**(4), 273–291.
14. Singh, K. K. K., Singh, K. B., Lokhande, R. D. and Prakash, A., Multielectrode resistivity imaging technique for the study of coal seam. *J. Sci. Ind. Res.*, 2004, **63**, 927–930.
15. Raja Rao, C. S., Coal resources of Tamil Nadu, Andhra Pradesh, Orissa and Maharashtra. *Bull. Geol. Surv. India, Ser. A., Coal-fields of India, II*, 1982, **45**, 9–40.
16. Goswami, S., Record of Lower Gondwana megafloral assemblage from Lower Kamthi Formation of Ib River Coalfield, Orissa, India. *J. Biosci.*, 2006, **31**(1), 115–128.
17. Geological report on detailed exploration of coal reserves in Talabira Block-I, IB Valley Coalfield, Odisha, vol. II, Central Mine Planning & Design Institute Limited (CMPDI), Ranchi, 1995.
18. Griffiths, D. H. and Barker, R. D., Two-dimensional resistivity imaging and modeling in areas of complex geology. *J. Appl. Geophys.*, 1993, **29**, 211–226.
19. Loke, M. H. and Barker, R. D., Rapid Least-square inversion of apparent resistivity pseudosections by a quasi-Newton method. *Geophys. Prospect.*, 1996, **44**, 131–152.
20. deGroot-Hedlin, C. and Constable, S., Occam's inversion to generate smooth, two-dimensional models from magnetotelluric data. *Geophysics*, 1990, **55**, 1613–1624.
21. Sasaki, Y., Resolution of resistivity tomography inferred from numerical simulation. *Geophys. Prospect.*, 1992, **40**, 453–464.
22. Loke, M. H., Electrical imaging surveys for environmental and engineering studies: a practical guide to 2-D and 3-D surveys, 2000, pp. 8–25.
23. Edwards, L. S., A modified pseudosection for resistivity and induced-polarization. *Geophysics*, 1977, **42**, 1020–1036.
24. Saad, R., Nawawi, M. N. M. and Mohamad, E. T., Groundwater detection in alluvium using 2D electrical resistivity tomography. *Electron. J. Geotech. Eng.*, 2012, **17**, 369–376.
25. Yang, C.-H., Tong, L.-T. and Yu, C.-Y., Integrating GPR and RIP methods for water surface detection of geological structures. *Terr. Atmos. Ocean. Sci.*, 2006, **17**(2), 391–404.
26. Guerin, R., Leachate recirculation: moisture content assessment by means of a geophysical technique. *Waste Manage.*, 2004, **24**(8), 785–794.
27. Hack, R., Geophysics for slope stability. *Surv. Geophys.*, 2000, **21**, 423–448.
28. Kneisel, C., Assessment of subsurface lithology in mountain environments using 2D resistivity imaging. *Geomorphology*, 2006, **80**, 32–44.
29. Chatterjee, R. and Paul, S., Application of cross-plotting techniques for delineation of coal and non-coal litho-units from well logs in Jharia Coalfield, India. *Geomaterials*, 2012, **2**, 94–104.
30. Verma, R. K. and Bhui, N. C., Use of electrical resistivity methods for study of coal seam in parts of Jharia Coalfield, India. *Geoexploration*, 1979, **17**, 163–176.

ACKNOWLEDGEMENTS. We thank S. Govindan, Director, Central Water and Power Research Station, Pune for encouragement and permission to publish the paper. We also thank the project authorities for help and cooperation during data collection.

Received 28 March 2014; revised accepted 23 September 2014

High mobility of aluminium in Gomati River Basin: implications to human health

Dharmendra Kumar Jigyasu¹, Rohit Kuvar²,
Nupur Srivastava¹, Sandeep Singh³,
Indra Bir Singh¹ and Munendra Singh^{1,*}

¹Centre of Advanced Study in Geology, University of Lucknow, Lucknow 226 007, India

²Department of Applied Geology, Dr Hari Singh Gour Vishwavidyalaya, Sagar 470 003, India

³Department of Earth Sciences, Indian Institute of Technology Roorkee, Roorkee 247 667, India

Aluminium (Al), an environmentally abundant and immobile element, has been studied for its mobility in the Gomati River Basin, a part of the Ganga Alluvial Plain, northern India. The dissolved Al concentrations in the Gomati River water and the Lucknow groundwater range over three orders of magnitude, from 14 to 77,861 ppb. In the Gomati River water, Al is classified as a moderately mobile element. Nearly 19% of Lucknow groundwater samples and all the Gomati River water samples have Al values above the permissible limit (200 ppb) recommended by the World Health Organization. Systematic multi-disciplinary study is urgently required to understand the geological association of high Al mobility with human health in the Ganga Alluvial Plain, one of the densely populated regions of the world.

Keywords: Aluminium mobility, Ganga Alluvial Plain, groundwater, human health.

ALUMINIUM (Al) is the third most abundant element in the Earth's crust. Generally, the chemical weathering of

*For correspondence. (e-mail: smunendra@gmail.com)